Quantitative Structure−Activity Relationship and Complex Network Approach to Monoamine Oxidase A and B Inhibitors

Lourdes Santana,*[,†] Humberto González-Díaz,[†] Elías Quezada,[†] Eugenio Uriarte,[†] Matilde Yáñez,[‡] Dolores Viña,[‡] and Francisco Orallo[‡]

Department of Organic Chemistry, Department of Pharmacology, Faculty of Pharmacy, University of Santiago de Compostela 15782, Spain

Received June 1, 2008

The work provides a new model for the prediction of the MAO-A and -B inhibitor activity by the use of combined complex networks and QSAR methodologies. On the basis of the obtained model, we prepared and assayed 33 coumarin derivatives, and the theoretical prediction was compared with the experimental activity data. The model correctly predicted 27 compounds, and most of the active derivatives showed IC_{50} values in the μM−nM range against both the MAO-A and MAO-B isoforms. Compound **14** shows the same MAO-A inhibitory activity (IC_{50} = 7.2 nM), as clorgyline used as a reference inhibitor and has the highest MAO-A specificity (1000-fold higher compared to MAO-B). On the other hand, compounds **24** (IC_{50} = 1.2 nM) and **28** (IC_{50} = 1.5 nM) show higher activity than selegiline (IC_{50} = 19.6 nM) and high MAO-B selectivity with 100-fold and 1600-fold inhibition levels, with respect to the MAO-A isoform.

Introduction

Mono amine oxidases (MAOs)[a] are flavoenzymes bound to the outer mitochondrial membrane and are responsible for the oxidative deamination of neurotransmitters and dietary amines.[1,2] Two isoforms, namely MAO-A and MAO-B, have been identified on the basis of their amino acid sequences, three-dimensional structure, substrate preference, and inhibitor selectivity.[3,4] MAO-A has a higher affinity for serotonin and noradrenaline, whereas MAO-B preferentially deaminates phenylethylamine and benzylamine. These properties determine the clinical importance of MAO inhibitors. Selective MAO-A inhibitors such as clorgyline (irreversible) and moclobemide (reversible) are used in the treatment of neurological disorders such as depression,[5,6] whereas the selective and irreversible MAO-B inhibitors such as selegiline and rasagiline are useful in the treatment of Parkinson's[7,8] and Alzheimer's diseases.[9,10]

All of these aspects have led to an intensive search for novel MAO inhibitors (MAOIs), and this effort has increased considerably in recent years. However, earlier MAOIs introduced into clinical practice were abandoned due to adverse effects, such as hepatotoxicity, orthostatic hypotension, and the so-called "cheese effect", which was characterized by hypertensive crisis.[11,12]

In recent years, a broad consensus has been reached concerning the necessity for a search for novel MAOIs and the study of their interaction with MAOs.[13−15] The major breakthrough has been brought about by the crystallization of hMAO-B with different inhibitors.[16] This fact explains the subsequent elucidation and determination of the 3D structure of the active site of hMAO-A[3] and opened new possibilities for the design of more selective and reversible drugs and facilitated the computer-assisted development of more selective inhibitors. Molecular docking calculations,[17,18] as well as comparative molecular field analysis (CoMFA)[19,20] and 3D quantitative structure−activity relationships (3D-QSAR),[21,22] are among the computational methods that have been used to predict MAOIs. Moreover, the estimation of docking parameters for lead drug candidates may involve time-consuming operations in which the interactions of large libraries of chemicals with different isoenzymes must be calculated. In the case of CoMFA, a critical step is the positioning and subsequent alignment of the molecules, a requirement that limits its applications to homogeneous series of compounds. Finally, 3D-QSAR methods also involve the time-consuming optimization of molecular geometry. Moreover, to the best of our knowledge, almost all models reported to predict MAOIs apply only to one series of compounds or ignore aspects such as the isoenzyme selectivity or the enzymatic source used in the experimental protocols (animal species and organs or tissues). As a result, for large and complex databases, the use of a combined QSAR and complex network approach can be considered as the most appropriate methodology in the search for new selective MAO inhibitors.

Almost all QSAR techniques are based on the use of molecular descriptors, which are numerical series' that codify useful chemical information and enable correlations to be made between statistical and biological properties.[23−26] The principal deficiency in the use of some molecular indices concerns their lack of physical meaning. In this respect, the introduction of novel molecular indices must obey physicochemical laws in order to ensure a theoretically rigorous interpretation of the results.[24]

In the particular case of MAOIs, electron delocalization and its consequences, such as polarizability and hydrophobicity, may be a determinant physical factor. This issue can be explained by considering that two models have been proposed for MAO catalysis, and these involve an electron transfer or a polar nucleophilic mechanism.[13,16,27] Our research group has just introduced a novel series of stochastic indices in the so-called Markov chains invariants for simulation and design (MARCH-INSIDE) approach. The method is based on the use of Markov

* To whom correspondence should be addressed. Phone: +34-981-563100. Fax: +34-981 594912. E-mail: qolsant@usc.es.

† Department of Organic Chemistry, Faculty of Pharmacy, University of Santiago de Compostela.

‡ Department of Pharmacology, Faculty of Pharmacy, University of Santiago de Compostela.

[a] Abbreviations: QSAR, quantitative structure−activity relationship; CN, complex networks; MAO, monoamine oxidase; MARCH-INSIDE, Markov chains invariants for simulation and design; MM, Markov models; PCA, principal components analysis; LDA, linear discriminant analysis; LOO, leave-one-out.

10.1021/jm800656v CCC: $40.75
Published on Web 10/04/2008

models (MM)[28] to codify useful chemical structure information in terms of molecular electron delocalization, polarizability, refractivity, and *n*-octanol/water partition coefficient.[29−31]

In previous work, we developed a MARCH-INSIDE methodology to seek a QSAR for MAO inhibitors.[32] This QSAR model was then used to predict the in vitro inhibitory MAO-A activity of a series of new coumarin derivatives. Most of the compounds were confirmed to be active, and one of these compounds (**18**) proved to have a very high activity (submicromolar range).

On the basis of the above information, in the work described here, we developed a new methodology in which we combined complex networks (CN) analysis with a QSAR methodology to carry out a unified analysis on a very large database. The work provides a method for the prediction of the MAO-A and/or -B inhibitory activity. The data set compiled and analyzed is possibly one of the largest and most up-to-date and includes ex vivo pharmacological activity information for heterogeneous series of compounds measured in cellular lines extracted from different organs (liver, brain, placenta, and platelets) of human, mouse, rat, baboon, as well as human in vitro data. Experimental conditions related to the isoenzyme (MAO-A or -B), the animal species and the organ were encoded with dummy variables. A very good MARCH-INSIDE-QSAR model was obtained, and the subsequent combined QSAR-CN analysis may become of major importance for the prediction of the MAO-A/B activity of new compounds.

Bearing in mind our experience in the field of coumarin compounds, the model was subsequently used to predict the MAO-A/B inhibitory activity of a designed library of coumarin derivatives, which were prepared and experimentally assayed as in vitro inhibitors using recombinant human MAO-A and MAO-B.

Results and Discussion

QSAR-CN Approach to MAO-A and/or -B Inhibitors. Our main focus in the QSAR study performed was to consider the differences in the inhibitory properties with MAOs from different animal species' and organs.[33,34] Hence, the development of a discriminant function[35] for the classification of organic compounds as MAO-A and/or MAO-B inhibitors (2 isoenzymes) in four animal species (human, bovine, mouse, and baboon) and using enzymes from four different origins (liver, brain, placenta, and platelets) is the key step in the present approach. We a selected a data set of 3408 cases. A case is defined as the activity class (inhibitor/nonactive) of one compound as an inhibitor of MAO-A and/or -B. As mentioned above, a compound may generate a number of statistical cases per drug (nscpd) equal to nscpd = (number of enzymes) × (number of animal species) × (number of organ of origins) = 2 × (4) × (4) = 32. Consequently, a compound with inhibitory activity reported for only one of the two enzymes, one of the animal species, and one of the organ targets generates only one statistical case (as found in almost all QSAR studies). In contrast, a compound with activity previously reported either for one, more than one, or none of the enzymes, species, and organs generates, respectively, zero or a number of statistical cases higher than 2 and lower than 32.

The structure/activity assay conditions (enzyme, animal species, enzyme organ of origin) and biological activity results for all cases were then encoded with continuous or dummy variables.

1. The chemical structures of compounds were encoded with continuous variables (global or local molecular descriptors) that were calculated using the MARCH-INSIDE approach.[31]

This method is based on the calculation of the different physicochemical molecular properties as an average of atomic properties (ap). For instance, it is also possible to derive average estimations of molecular or group electronegativities (${}^k\chi$), molar refractivities (^{k}MR), polarizabilities (${}^k\alpha$), water/*n*-octanol partition coefficients ($\log {}^kP$), and atomic van der Waals volumes (${}^kV_{vdw}$).

It is possible to consider isolated atoms ($k = 0$) in the estimation of the molecular properties. In this case, the probabilities ${}^0p(\mathrm{ap}_j)$ are determined without considering the formation of chemical bonds (simple additive scheme). However, it is possible to consider the gradual effects of the neighboring atoms at different distances in the molecular backbone. To achieve this goal, the method uses a MM, which determines the absolute probabilities ${}^kp(\mathrm{ap}_j)$ with which the atoms placed at different distances k affect the contribution of the atom j to the molecular property in question.

Finally, it is interesting to note that one can sum only the atoms included in a specific group (G) rather than all atoms. In this way we can approach specific classes of average properties such as average electronegativity for sp_3 carbon atoms (C_{sp3}) or average polarizability for heteroatoms (Het). The number of chemical groups used was four and includes the following: heteroatoms (Het), heteroatom-bonded hydrogens (H-Het), saturated carbon atoms (C_{Sp3}), unsaturated carbon atoms ($C_{Sp\&Sp2}$). The number of topological distances k between atoms considered for calculations was six, including 0, 1, 2, 3, 4, and 5. In total, we calculated a number of molecular descriptors per molecule $5 \times (4 + 1) \times 6 = 150$, the 1 in the formula accounts for the molecule as a whole. This means that we represented the molecular structure of each molecule by a vector with 150 components (global and local molecular descriptors).

2. The biological data and activity assay conditions were also considered. The dummy or coding variables assign two possible values (e.g., 1 and 0) when the case presents a certain condition. We used dummy variables either as inputs or as outputs of the model. The variable MAO (A/B)i-score is the output of the model, i.e., the variable to be predicted by the QSAR. This variable is 1 when a compound was experimentally confirmed as an inhibitor of the corresponding enzyme for a given organ and species and −1 otherwise. We also used dummy variables as inputs of the model to indicate precisely the conditions of the experiment (animal species or organ of origin). The input dummy variables used were MAO enzyme ($A = 1$, $B = 0$), liver, brain, placenta, platelets, mouse, human, baboon, and bovine in this order from left to right in the data source file (see Supporting Information file). In closing, a case in the data is represented by 9 conditions + 150 descriptors = 159 input values and 1 output value.

To reduce the dimensionality of the problem, we conducted a PCA analysis. We calculated up to 10 principal components or factors (Fs), which were later used as inputs for the QSAR analysis. PCA and classification scores allowed us to select at random the training and validation series' of compounds. This group contains chemicals with IC_{50} values ≤ 25 μM or, in some cases, compounds that show an inhibition percentage of $\geq 50\%$ at inhibitor concentrations ≤ 25 μM. This series is composed at random by the most representative families of MAO-A/B inhibitors taken from the literature (Supporting Information); these include propargyl derivatives, benzamides, phenylethylamines, indoles, coumarins, thioxanthenes, oxadiazolidones, and diazoheterocyclic compounds. The remaining compounds were a heterogeneous series of inactive compounds including members of the aforementioned families, with $IC_{50} > 25$ μM, along

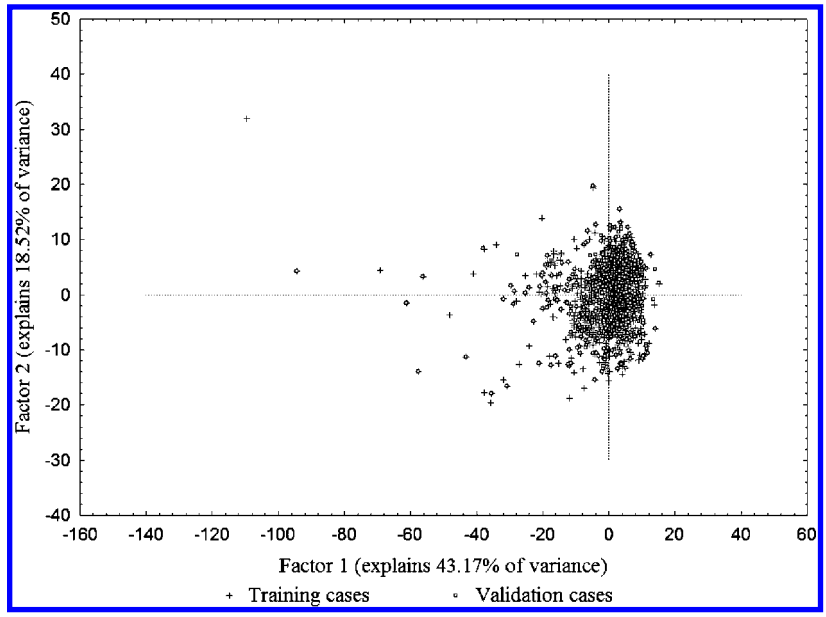

Figure 1. PCA plot for training and validation cases. Note that almost all cases lie within the principal cloud of points; note also the main axes that define the four quadrants.

with many other structural patterns extracted from international databases.[36,37] It is common for compounds with even higher IC_{50} values to be considered as active or moderately active, but we considered 25 μM to be a reasonable limit. The selection of higher break point values to cluster chemicals by their MAO-A/B IC_{50} may generate a series with a clearly disproportionate size and, therefore, a vastly reduced number of active compounds. The selection here of discriminant techniques instead of regression techniques was determined by the lack of homogeneity in the conditions under which these values were measured. As reported in different sources, numerous IC_{50} values lie within a range rather than a single value. In other cases, the activity is not scored in terms of IC_{50} values but is quoted as inhibitory percentages at a given concentration.

The PCA scores for all cases were depicted in a plot of the first factor F_1 versus F_2. These factors are the most important, and together they explain a cumulative variance of F_1 (explained variance) + F_2 (explained variance) = 43.17 + 18.52 = 61.69% of the total variance. For training and validation, we selected at random compounds that lie within the four quadrants of the cloud of points. The overall distribution of compounds in this plot is illustrated in Figure 1. Once the training series had been designed, forward stepwise linear discriminant analysis (LDA) was carried out in order to derive the QSAR for the MAO-A/MAO-B inhibitory activity score MAO(A,B)i:

$$\text{MAO(A, B)}i - \text{score} = 0.14 \cdot F_1 + 0.56 \cdot F_2 + 0.40 \cdot F_3 - 0.02$$
$$Rc = 0.79 \quad U = 0.38 \quad p < 0.001 \tag{1}$$

The statistical significance of this model was determined by examining the canonical regression coefficient (*Rc*), the *U*-statistic (which is also known as Wilk's λ statistic), and the *p*-level (*p*). We also inspected the percentage of good classification in training and validation experiments. Overall, the model correctly classified 3222 out of 3408 inputs (94.5%).

This includes the correct prediction of 1481 out of 1501 results for experimental assays of MAO-A and/or MAO-B inhibitors (98.7%) and 1741 out of 1907 nonactive compounds. Briefly, training classification and external validation rates were above 90% for all positive/negative groups in training/validation series. Details of this information are provided in Table 1. In addition to these results, the linear relationship between leave-one-out (LOO) residuals and raw residuals are shown in Figure 2, and these also illustrate the high stability of the model to data variation.

Table 1. Training and Validation Results for the MAO Inhibitors QSAR

%		nonactive	MAO inhibitors
	Train		
90.8	nonactive	1300	131
98.7	MAO inhibitors	15	1119
94.3	total		
	Validation		
92.6	nonactive	441	35
98.6	MAO inhibitors	5	362
95.3	total		
	Both		
91.3	nonactive	1741	166
98.7	MAO inhibitors	20	1481
94.5	total		

The results strongly validate the model as a predictor of appropriate interactions of a selected compound as an MAO-A and/or MAO-B inhibitor. The model is able to predict for a new compound one probability value for each of the possible outputs including assays in cellular lines extracted from different organs (liver, brain, placenta, and platelets) of human, mouse, rat, and baboon species. The results for a selected group of compounds are given in Table 2. For detailed information on all compounds used, see Tables 1SI, 2SI, and 3SI in the online Supporting Information.

The values of the PCA scores for each compound weighted with the LDA-QSAR model coefficients were used to calculate a very large matrix of compound−compound pairwise Euclidean distances. After selection of a cutoff value, this matrix was transformed into a Boolean (0, 1) matrix. The matrix can be represented as a very large graph or network that expresses the similarity/dissimilarity relationships of very heterogeneous

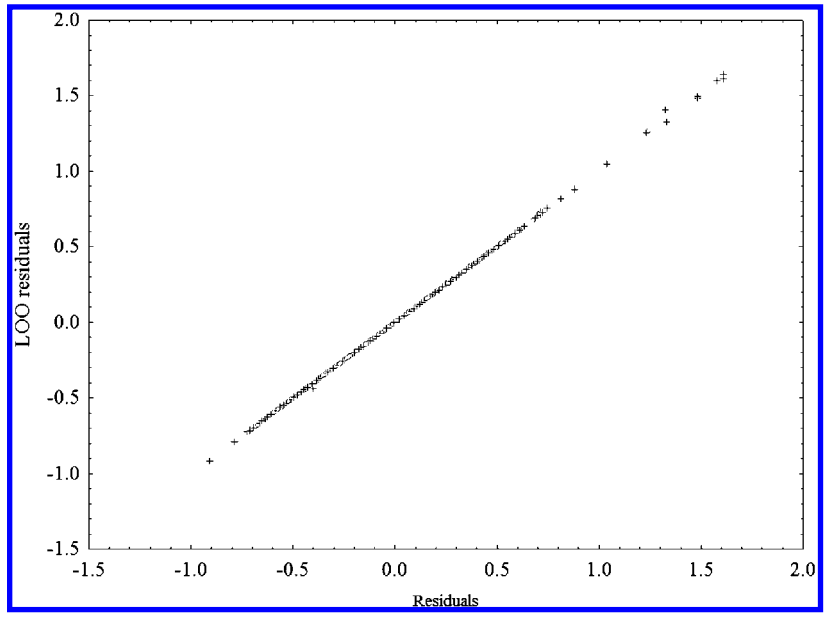

Figure 2. Model robustness to LOO variation of the data.

Table 2. Prediction of the Interaction with MAO-A and/or MAO-B Isoenzymes for a Selected Group of Compounds[a]

compds	ref	N^b	OC[c]	PC[c]	P^d	t/cv[e]	F_1[f]	F_2[f]	F_3[f]	MAO	organ	species
isoquinolin42	51	25	1	1	0.53	t	9.17	−2.58	0.13	B	liver	human
isoquinolin42	51	25	1	1	0.54	t	9.26	−2.48	0.00	A	placenta	human
oxazolinon25	57	2j	1	1	0.58	t	3.12	−2.03	2.04	A	brain	bovine
oxazolinon25	57	2j	1	1	0.59	cv	3.11	−2.02	2.04	B	brain	bovine
quinaz40	82	37	1	1	0.95	cv	−3.34	4.70	1.65	A	platelets	human
quinaz40	82	37	1	1	0.95	cv	−3.35	4.71	1.66	B	platelets	human
tetrazole27	37	17g	1	1	0.89	t	−1.08	2.84	1.07	A	brain	mouse
tetrazole27	37	17g	1	1	0.89	cv	−1.08	2.84	1.08	B	brain	mouse
						Nonactive Compounds						
amphetamin30	4	17	−1	−1	0.22	cv	6.47	−1.41	−4.06	A	brain	mouse
amphetamin30	4	17	−1	−1	0.22	t	6.47	−1.40	−4.05	B	brain	mouse
cypropamine9	43	3a	−1	−1	0.13	cv	6.57	−3.37	−2.97	A	liver	human
cypropamine9	43	4a	−1	−1	0.13	t	6.57	−3.36	−2.96	B	liver	human
indol4	46	6	−1	−1	0.33	t	8.71	1.37	−7.27	A	placenta	human
indol4	46	6	−1	−1	0.34	t	8.70	1.40	−7.24	B	platelets	human
indol16	48	4a	−1	−1	0.09	t	4.17	−1.52	−5.54	A	brain	bovine
indol16	48	4a	−1	−1	0.09	t	4.17	−1.52	−5.53	B	brain	bovine
proparg38	64	15	−1	−1	0.10	t	3.54	−8.03	4.05	A	liver	mouse
proparg38	64	15	−1	−1	0.11	t	3.54	−8.02	4.06	B	liver	mouse

[a] See Tables 1SI, 2SI, and 3SI of Supporting Information for detailed information of all compounds. [b] Number of each compound in the corresponding reference (Supporting Information). [c] Observed classification (OC) and predicted classification (PC); 1 for active, −1 for nonactive. [d] Subsequent probability of a positive activity predicted for each compound. [e] Train and cross-validation indicator, t for compounds in training and cv for compounds in the external validation series. [f] Factor scores (F_1 to F_3) for each compound.

classes of MAO-A and/or -B inhibitors in different mammalian species. This complex network is represented in Figure 3.

The topological parameters of the present network are very similar to the more typical free scale topology parameters. A number of interesting parameters to characterize the topology of this network and to compare it to a free scale topology are shown in Table 3. It can be seen that despite differences in some topological parameters, the network developed here perfectly fits to a power law distribution with a regression coefficient higher than 0.9. This kind of topology is characteristic of a network with a group of drugs called hubs (very connected nodes) that is representative of the vast universe of drugs considered. As a consequence, our network will very probably associate every new compound to one of these hubs. This combined QSAR-CN analysis may therefore become of major importance for the prediction of the binding of new compounds that could help to explain the nature of interactions. The clustering of the MAO-B inhibitors *N*-[4-[(3-fluorophenyl)-methoxy]phenyl]-5-*oxo*-3-pyrrolidinyl acetamide (pyrrolidone40) and *N*-[4-(3-fluoro-benzyloxy)-phenyl]-2-*oxo*-3-pyrrolidinylacetamide (pyrrolidone70)[38,39] using CentiBin software is represented in Figure 4. These compounds are similar only to 1 and 3 other drugs (see node degree centrality in the right-hand column of the figure), respectively, but pyrrolidone70 is similar to 2-fluoro-*N*-[4-[(3-fluorophenyl)methoxy]phenyl]-5-*oxo*-3-pyrrolidinylacetamide (pyrrolidone43) and *N*-[-5-*oxo*-4-[(2,4,6-trifluorohenyl)methoxy]henyl]-3-yrrolidinylacetamide (pyrrolidone52), which are typical pyrrolidone scaffold MAO-B inhibitors.[38] Both pyrrolidone43 and pyrrolidone52 are similar to more than 10 compounds (considering only the compounds depicted in this subnetwork). These latter two compounds are therefore candidates to be considered as drug-hubs that are characteristics of this class.

Rational Design and in Silico Evaluation of Novel Series of MAO-A and/or MAO-B Inhibitors. The model developed in this study was used for the design of novel MAO-

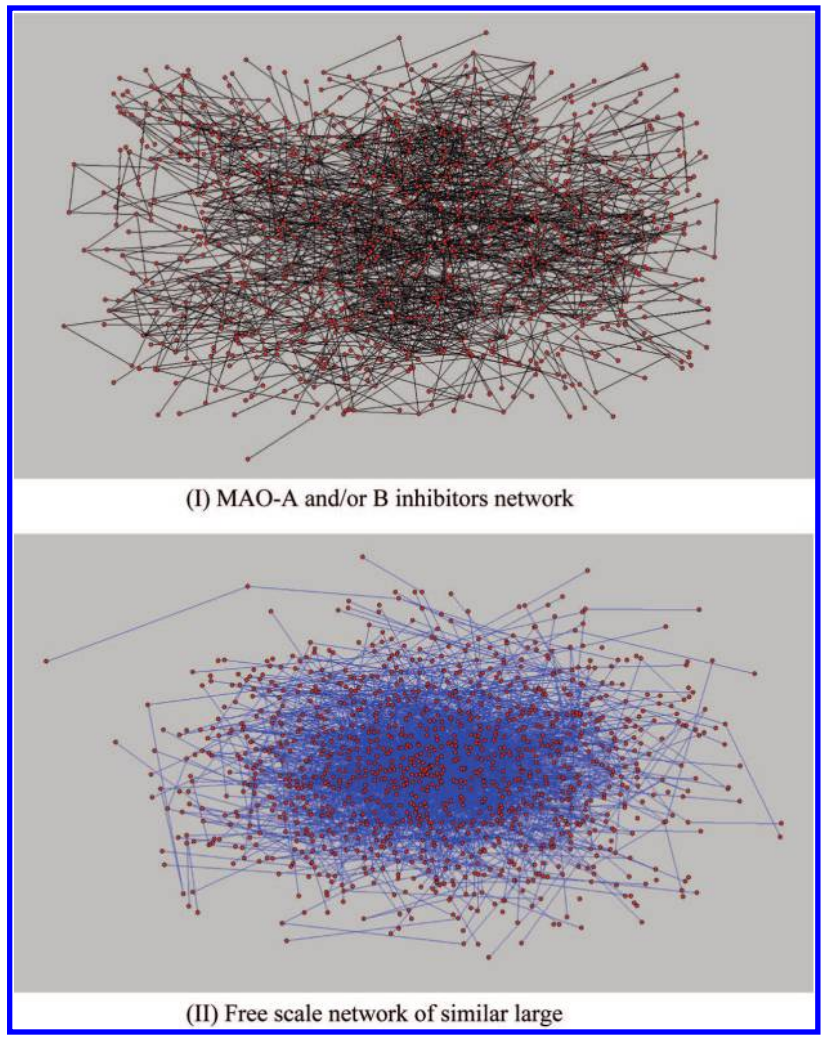

Figure 3. Free Kamada−Kawai visualization of the similarity/dissimilarity network for MAO-A and/or MAO-B inhibitors (I) and a free scale random network (II) for visual comparison purposes.

A/B inhibitors. As described previously, a specific way to new lead discovery involves several general common steps when used in terms of a QSAR: (a) construction of a suitable molecular database of compounds that either show the property in question or do not, (b) calculation of the molecular descriptors, (c) construction of the model, (d) estimation of the biological activity using QSAR, (e) synthesis and characterization of selected compounds, and (f) assay of the candidate compounds in order to corroborate the predicted biological activity.

The coumarin analogues are a family of natural and/or synthetic compounds with different pharmacological activities, one of which is MAO inhibitory activity.[40,41] In many cases, it is known that activity and selectivity are determined by the nature of the substituents at the 7- and the 4/3-positions.[42−44] On the other hand, in a previous investigation,[32] we developed QSAR studies for the MAO-A inhibitory activity in a series of coumarin derivatives and found that the most active compounds were the 7-acetonyloxy-substituted compounds, which showed higher activity than their cyclic analogues and were also more active than the 7-hydroxy precursors.

On the basis of the above information, and with the aim of exploring the structure-affinity and MAO-A/B selectivity relationships, in the present work, we designed a series of 33 coumarin derivatives (Table 4) that include the aforementioned chemical diversity with particular attention paid to the most interesting 7-(β-ketoether)coumarin derivatives. The compounds were synthesized according to Scheme 1, and details are given in the Experimental Section.

Chemistry. The coumarin derivatives **8**, **9**, **11**, **13**−**15**, **21**, **22**, **24**−**29**, **32**, and **33** were efficiently synthesized according to the synthetic protocol outlined in Scheme 1. The remaining compounds were prepared as reported in our previous communications.[32,45−47]

Pechmann condensation of 2-alkyl resorcinol with the corresponding ketoester afforded the 3,4-cyclopentene/cyclohexene-7-hydroxy coumarins **8** and **9**. The Williamson reaction of the 7-hydroxycoumarins **1**−**3**, **8**, and **9** with 2-chloroketones or 2,3-dibromopropene gave the corresponding ethers **11**, **13**−**15**, **21**, **22**, **24**, and **25**. Compounds **22**, **23**, and **25** were oxidized with DDQ to give the corresponding 3,4-benzocoumarin derivatives **26**−**28**. Finally, cyclization of coumarin ketoethers **11**, **14**, and **15** in strongly alkaline solution led to the furanocoumarins **29**, **32**, and **33**.

MAO Inhibition Assay. The potential effects of the test drugs on hMAO activity were investigated by measuring their effects on the production of hydrogen peroxide from *p*-tyramine (a common substrate for both hMAO-A and hMAO-B), using the 10-acetyl-3,7-dihydroxyphenoxazine as reagent and microsomal MAO isoforms prepared from insect cells (BTI-TN-5B1-4) infected with recombinant baculovirus containing cDNA inserts for hMAO-A or hMAO-B.

Table 3. Comparative Study of MAO-A and/or -B Inhibitors Network and Free-Scale Topology

networks	MAOi (I)	scale free (II)
Classic Topological Properties		
number of nodes (drugs): n	1174	1174
number of arcs (similar drug−drug pairs): m	3873	2921
average node degree (similar drugs)	2.6	5.0
average drug−drug Euclidean distance	2.7	
average drug−drug topological distance		4.2
max m possible: max$m = n!/(n-2)!\cdot 2!$	688551	688551
edge density[a]	**0.6**	**0.4**
Free-Scale Typical Properties for Semilog$_{10}$ Plot of Distribution Histogram		
free-scale regression coefficient: R	**0.95**	**0.99**
average value	1.24	1.55
standard deviation	0.02	0.36
Other Important Topological Properties		
Zagreb group index 1: M1	99452	60328
Zagreb group index 2: M2	938872	352307
Randic connectivity index: Xr	583.5	435.9
Platt index: F	91706	54486
index of relinking: P	1.99	1.94

[a] The drug-to-drug average Euclidean distance could not be determined for the scale free network because the generation of this network with Pajek omits the Euclidean distance step. Average topological distance could not be calculated for MAOi-QSAR network with CentiBin due to loss of connectivity; however, edge density I is slightly higher than edge density II. Consequently, we can conclude that the average distance for network I is only slightly lower than the average distance of the free scale network.

The production of H_2O_2 catalyzed by MAO isoforms can be detected using the previously mentioned reagent, a nonfluorescent, highly sensitive, and stable probe that reacts with H_2O_2 in the presence of horseradish peroxidase to produce a fluorescent product, resorufin. In this study, hMAO activity was evaluated using the above method following the general procedure described previously by us.[48]

The tested drugs (new compounds and reference inhibitors) inhibited the control enzymatic MAO activities and the inhibition was concentration dependent. The corresponding IC_{50} values and MAO-B selectivity ratios [IC_{50} (MAO-A)]/[IC_{50} (MAO-B)] are shown in Table 5.

The assayed compounds themselves do not react directly with the 10-acetyl-3,7-dihydroxyphenoxazine, which indicates that these drugs do not interfere with the measurements.

In our experiments and under our experimental conditions, hMAO-A displayed a Michaelis constant (K_m) of 457.17 ± 38.62 μM and a maximum reaction velocity (V_{max}) of 185.67 ± 12.06 nanomol/min/mg protein, whereas hMAO-B showed a K_m of 220.33 ± 32.80 μM and a V_{max} of 24.32 ± 1.97 nanomol/min/mg protein ($n = 5$).

Conclusions

In this study, we have developed a QSAR-CN analysis for the design of novel MAO inhibitors using a very large database of heterogeneous compounds and their activities measured in cellular lines from different organs and species. The model correctly classified 3222 out of 3408 inputs (94.5%) and was then used to predict the activity of 33 compounds in our designed coumarin library. All of the active compounds were correctly predicted by the model, and a total of 27 (81.82%) and 24 (72.73%) compounds were correctly predicted as MAO-A and MAO-B inhibitors, respectively.

On the other hand, the SAR analysis seems to corroborate the importance of the structural requirements of the substituents in the coumarin moiety in order to achieve good activity and MAO-A/B selectivity, as indicated in the literature.[42−44] The 7-hydroxy derivatives have been shown to be inactive, even with the introduction of bulky substituents in any other positions of the coumarin (compounds **1**−**10**). The introduction of acetonyl/bromoallyloxy groups in the 7-position of the coumarin yielded compounds (**11**−**28**) with greater MAO-A and MAO-B inhibitory activity. The cyclization of this group or the formation of the furocoumarin analogues (**29**−**33**) again resulted in a reduction of both MAO-A and MAO-B iso-enzyme inhibitory activities with respect to the acyclic analogues. Finally, the most relevant findings are that: (a) the introduction of bulky groups in the 7-acetonyl substituent increase MAO-A selectivity (**13**−**19**), (b) introduction of bulky groups such as cyclohexyl or phenyl in the 3,4-positions of the 7-acetonyl derivatives increased both MAO-A and MAO-B inhibitory activities with concomitant loss of selectivity, whereas replacement of the acetonyl substituent at position 7 by the bromoallyloxy group resulted in compounds **24** and **28**, which had very high MAO-B inhibitory activity (IC_{50} of about 1.2 and 1.5 nM) and the highest MAO-B selectivity (approximately 100-fold and 1600-fold) with respect to the MAO-A isoform.

In summary, we have developed good theoretical QSAR-CN models to predict inhibitory MAO activity. On the basis of this model, we have found new coumarin derivatives with inhibitory activity comparable to those of clorgyline and selegiline, respectively, which are used as reference inhibitors and have a very high MAO-A and MAO-B selectivity. These findings have encouraged us to continue our investigations into the design of more potent and selective analogues by introducing appropriate substituents into the coumarin scaffold.

Experimental Section

Computational Methods Used for QSAR-CN Analysis. The calculation of the molecular descriptors was implemented in the in-house software MARCH-INSIDE.[49]

To perform the multispecies activity analysis with a CN approach we carried out the following steps:

1. We calculated the weighted principal component loadings (multiplying the coefficients of the QSAR equation by the factor value included in the QSAR equation) for a large number of selected drugs; in the calculations, we included MAO-A and/or -B inhibitors assayed for at least one of the animal species and organs of origin studied.

2. All of the loadings were used as inputs for the STATISTICA software[50] employed to calculate drug−drug multispecies dissimilarities in the form of weighted Euclidean distances (w*Ed*). The values can be arranged in the form of a Euclidean distance matrix of drugs vs STATISTICA drugs. Each drug may appear more than once depending on the different assays reported for the particular drug.

3. Microsoft Excel was used to transform the drug pair distances matrix derived with Statistica into a Boolean matrix. The elements of this matrix are equal to 1 if two drugs tested under given conditions have a short w*Ed*, or the same if the QSAR-predicted results for these drugs in this test are very similar The threshold or cutoff value used was a distance of 0.005. The line command used in Excel to transform the distance matrix into a Boolean matrix was $f =$ if (A$1=$B2,0, if (B2>0.0051, 0, 1)). This allows the transformation of distance into Boolean values and makes the main diagonal elements 0 while avoiding loops in the future network. The Boolean matrix was saved as a.txt format file.

4. After renaming the.txt file as a.mat file, it was read with the software CentiBin.[51] The software can be used not only to represent the network but also to highlight all drugs (nodes) connected to a specific drug and to calculate numerous parameters including node degree (the number of drugs with similar predicted results).

5. Pajek software[52] submenu parameters, which appear in the bar menu option network information, were used to request the

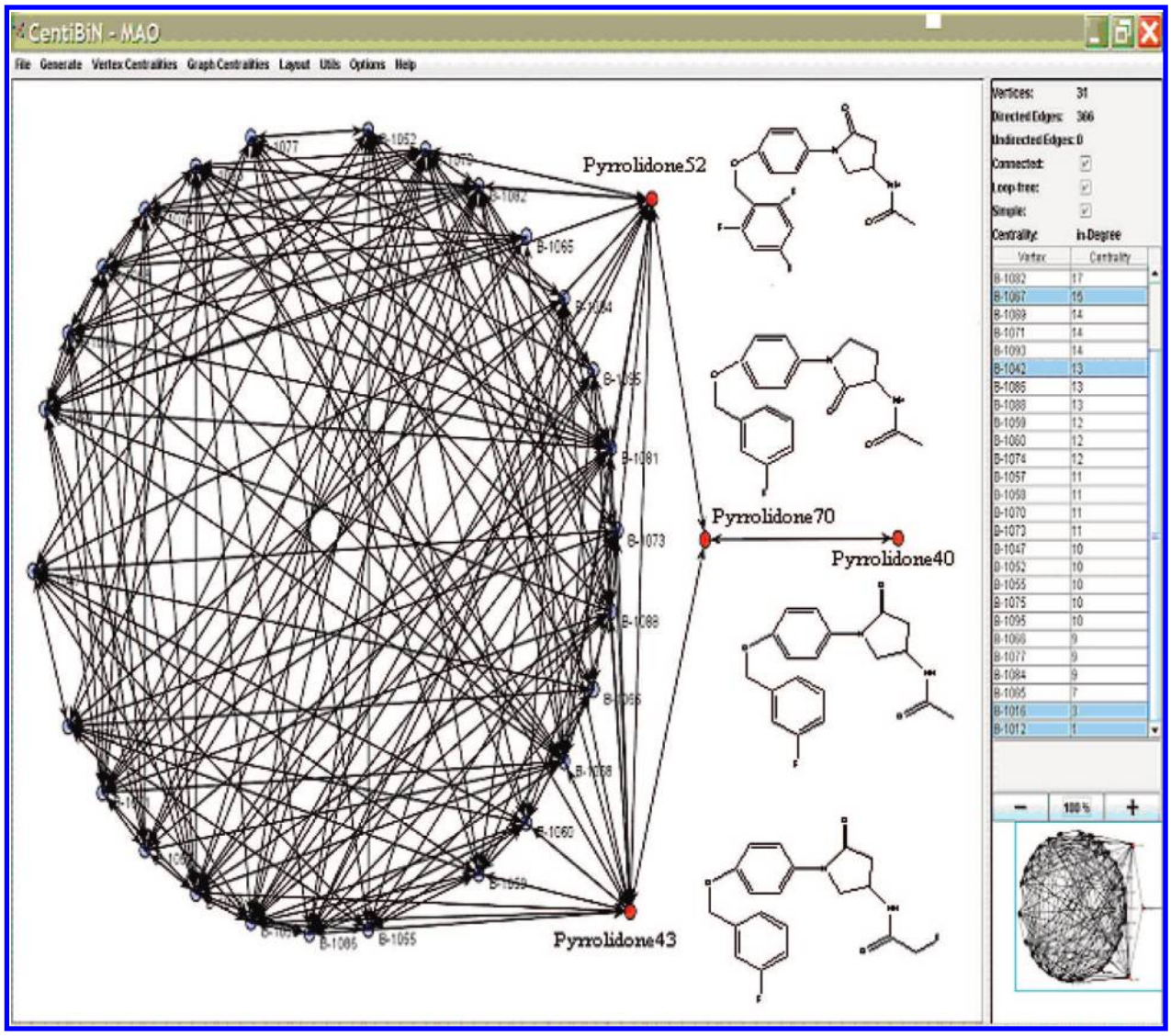

Figure 4. View of a subnetwork corresponding to a cluster of MAO-B inhibitors that exemplify the identification of a compound with a pyrrolidine scaffold with other similar analogues.

calculation of several parameters that describe network topology including: Zagreb group M1 and M2 indices, Platt index *F*, Randic connectivity index *Xr*, and index of relinking. We used these parameters to compare the topology of the network constructed by QSAR for MAO inhibitors with a free scale random network. We generated this random network with Pajek, containing the same number of nodes (drugs) as our network.

Chemistry. Melting points were determined using a Reichert Kofler thermopan or in capillary tubes on a Büchi 510 apparatus and are uncorrected. IR spectra were recorded on a Perkin-Elmer 1640FT spectrophotometer. ^{1}H and ^{13}C NMR spectra were recorded on a Bruker AMX spectrometer at 300 and 75.47 MHz, respectively, using TMS as internal standard (chemical shifts in δ values, *J* in Hz). Mass spectra were obtained using a Hewlett-Packard 5988A spectrometer. Elemental analyses were performed using a Perkin-Elmer 240B microanalyzer and were within ± 0.4% of calculated values in all cases. Silica gel (Merck 60, 230−00 mesh) was used for flash chromatography (FC). Analytical thin layer chromatography (TLC) was performed on plates precoated with silica gel (Merck 60 F254, 0.25 mm).

General Procedure for the Preparation of 3,4-Cycloalkane-7-hydroxycoumarins (8, 9). 2-Methylresorcinol (80.554 mmol) was dissolved in 12 M H_2SO_4 (120 mL). The appropriate ethyl 2-oxocycloalkanecarboxylate (96.65 mmol) was added, and the solution was stirred at room temperature for 15 h. The reaction mixture was then poured into ice/water (100 mL), and the precipitate was recovered by filtration and washed with water to yield the desired compound, which was purified by crystallization.

8-Methyl-3,4-cyclopentene-7-hydroxycoumarin (8). Yield 82%; mp 259 °C (EtOH). ^{1}H NMR (DMSO-d_6) 2.07 (m, 2H, $CH_2C\underline{H}_2CH_2$), 2.16 (s, 3H, Me-C8), 2.70 (t, J = 7.3, 2H), 2.98 (t, J = 7.5, 2H), 6.84 (d, J = 8.4, 1H, H-6), 7.24 (d, J = 8.4, 1H, H-5), 10.30 (s, 1H, OH). ^{13}C NMR (DMSO-d_6) 8.21 (Me-C8), 22.03 ($CH_2\underline{C}H_2CH_2$), 29.88, 31.60, 110.57 (C8), 110.63, 111.66 (C6), 121.89, 123.00 (C5), 153.35, 157.02, 158.25, 159.46 (C2). IR 3362, 2920, 1682, 1577, 1275, 1081, 812. MS *m*/*z* 217 ([M + 1]$^+$, 14), 216 (M$^+$, 100), 188 (58), 187 (65), 145 (6), 128 (3). Anal. ($C_{13}H_{12}O_3$) C, H.

8-Methyl-3,4-cyclohexene-7-hydroxycoumarin (9). Yield 71%; mp 279−280 °C (EtOH). ^{1}H NMR (DMSO-d_6) 1.69 (m, 4H, $CH_2(C\underline{H}_2)_2CH_2$), 2.11 (s, 3H, Me-C8), 2.35 (m, 2H), 2.64 (m, 2H), 6.79 (d, J = 8.6, 1H, H-6), 7.30 (d, J = 8.6, 1H, H-5), 10.16 (s, 1H, OH). ^{13}C NMR (DMSO-d_6) 8.30 (Me-C8), 21.29, 21.61, 23.78 ($\underline{C}H_2$−C4), 24.95, 110.61 (C8), 111.87 (C6), 112.25, 118.27, 121.78 (C5), 148.13, 151.40, 157.94, 161.45 (C2). IR 3275, 2932, 1676, 1606, 1374, 1266, 1102, 804. MS *m*/*z* 231 ([M + 1]$^+$, 15), 230 (M$^+$, 100), 215 (47), 202 (33), 174 (60). Anal. ($C_{14}H_{14}O_3$) C, H.

General Procedure for the Preparation of Oxoether Derivatives 11, 13−15, 21, 22, 24, and 25. To a solution of the substituted 7-hydroxycoumarin derivatives **1**−**3**, **8**, or **9** (62 mmol) in dry acetone (300 mL) were added K_2CO_3 (4 g) and the corresponding 2-chloroketones or 2,3-dibromopropene (120 mmol). The mixture

Table 4. Structure of the Coumarin Derivatives **1**−**33**

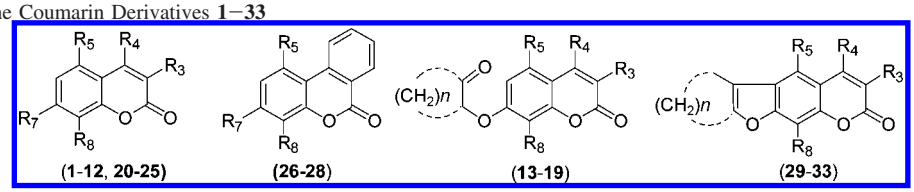

compd	R_3	R_4	R_5	$R_7/(CH_2)n$	R_8
1	H	H	OMe	OH	H
2	H	Me	H	OH	OMe
3	H	Me	H	OH	Me
4	H	Me	H	OH	H
5	NH_2	H	H	OH	OMe
6	$-(CH_2)_3-$		H	OH	H
7	$-(CH_2)_3-$		H	OH	OMe
8	$-(CH_2)_3-$		H	OH	Me
9	$-(CH_2)_4-$		H	OH	Me
10	$-(CH_2)_4-$		H	OH	OMe
11	H	H	OMe	$MeCOCH_2O-$	H
12	NHAc	H	H	$MeCOCH_2O-$	OMe
13	H	H	H	$-(CH_2)_3-$	OMe
14	H	H	H	$-(CH_2)_3-$	Me
15	H	H	H	$-(CH_2)_4-$	Me
16	H	H	OMe	$-(CH_2)_4-$	H
17	H	Me	H	$-(CH_2)_4-$	OMe
18	H	Me	H	$-(CH_2)_3-$	H
19	H	H	H	$-(CH_2)_4-$	H
20	$-(CH_2)_3-$		H	$MeCOCH_2O-$	OMe
21	$-(CH_2)_3-$		H	$MeCOCH_2O-$	Me
22	$-(CH_2)_4-$		H	$MeCOCH_2O-$	Me
23	$-(CH_2)_4-$		H	$MeCOCH_2O-$	OMe
24	$-(CH_2)_3-$		H	$CH_2C(Br)CH_2-$	Me
25	$-(CH_2)_4-$		H	$CH_2C(Br)CH_2-$	Me
26	Ph		H	$MeCOCH_2O-$	Me
27	Ph		H	$MeCOCH_2O-$	OMe
28	Ph		H	$CH_2C(Br)CH_2-$	Me
29	H	H	OMe		H
30	NH_2	H	H		OMe
31	H	H	H	$-(CH_2)_2-$	H
32	H	H	H	$-(CH_2)_2-$	Me
33	H	H	H	$-(CH_2)_3-$	Me

Scheme 1. Synthetic Strategy for Prepared Compounds

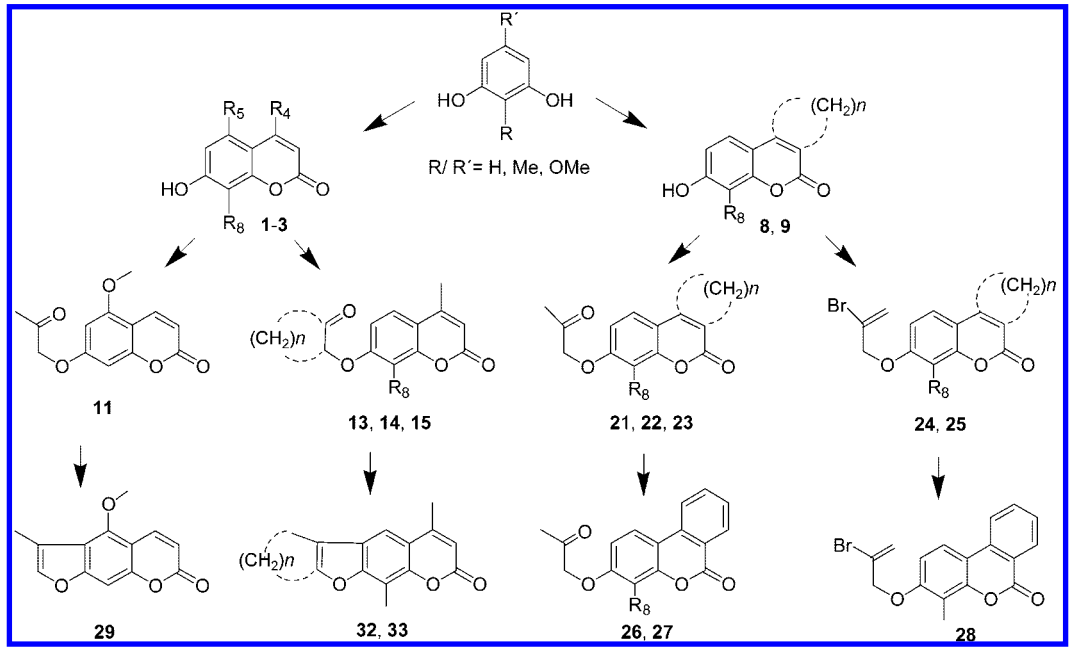

was heated under reflux for 24 h. The mixture was cooled, and the solid residue was filtered off. The solvent was removed under reduced pressure, and the crude product was purified by FC and/or crystallization to give the desired compound.

7-Acetonyloxy-5-methoxycoumarin (11). Yield 77%; mp 160 °C. ^{1}H NMR ($CDCl_3$) 2.30 (s, 3H, Me-CO), 3.91 (s, 3H, MeO), 4.63 (s, 2H, CH_2O), 6.19 (d, J = 9.7, 1H, H-3), 6.29 (d, J = 2.1, 1H, H-6), 6.38 (d, J = 2.1, 1H, H-8), 7.97 (d, J = 9.7, 1H, H-4). ^{13}C

Table 5. In Vitro and in Silico Evaluation of MAO Inhibitory Activities of Compounds **1**−**33** and Reference Inhibitors[a]

				MAO-A			MAO-B		
compd	MAO-A IC_{50}	MAO-B IC_{50}	MAO-A/B	obsd[f]	predicted[f]	P[e]	obsd[f]	predicted[f]	P[e]
1	**	**	–	–	–	0.38	–	–	0.38
2	80.30 ± 5.82 μM	**	<0.80[d]	–	–	0.22	–	–	0.22
3	**	71.32 ± 3.17 μM	>1.40[d]	–	–	0.40	–	–	0.41
4	**	80.41 ± 5.16 μM	>1.24[d]	–	–	0.48	–	–	0.49
5	**	**	–	–	–	0.37	–	–	0.08
6	48.20 ± 3.61 μM	**	<0.48[d]	–	–	0.33	–	–	0.33
7	63.53 ± 3.72 μM	**	<0.63[d]	–	–	0.26	–	–	0.26
8	>**	**	–	–	–	0.29	–	–	0.29
9	60.11 ± 3.47 μM	**	<0.60[d]	–	–	0.27	–	–	0.27
10	**	50.20 ± 1.49 μM	>1.99[d]	–	–	0.26	–	–	0.26
11	**	44.10 ± 2.80 μM	>2.27[d]	–	+	0.83	–	+	0.83
12	5.31 ± 0.12 μM	**	<0.53[d]	+	+	0.85	–	+	0.69
13	2.66 ± 0.18 μM[b]	856 ± 19.50 μM	0.0031	+	+	0.87	–	+	0.87
14	7.16 ± 0.52 nM[b]	10.60 ± 0.96 μM	0.00067	+	+	0.87	+	+	0.88
15	0.40 ± 0.03 μM[b]	3.87 ± 0.15 μM	0.10	+	+	0.87	+	+	0.87
16	20.35 ± 1.12 μM	***	<0.41[d]	+	+	0.72	–	–	0.42
17	15.45 ± 0.56 μM	***	<0.31[d]	+	+	0.72	–	+	0.72
18	40.50 ± 2.2 nM[b]	5.57 ± 0.32 μM	0.0073	+	+	0.83	+	+	0.83
19	43.00 ± 2.93 μM	**	<0.43[d]	–	+	0.71	–	+	0.80
20	121 ± 7.43 nM[b]	12.98 ± 0.91 μM	0.0093	+	+	0.68	+	+	0.68
21	235 ± 18.52 nM[c]	165 ± 7.04 nM	1.42	+	+	0.71	+	+	0.71
22	3.78 ± 0.34 nM[b]	17.3 ± 1.48 μM	0.22	+	+	0.69	+	+	0.69
23	396 ± 16.63 nM[b]	12.12 ± 1.03 μM	0.033	+	+	0.66	+	+	0.66
24	130 ± 11.77 nM[b]	1.18 ± 0.15 nM	110	+	+	0.94	+	+	0.94
25	695 ± 28.54 nM[c]	236 ± 5.03 nM	2.94	+	+	0.94	+	+	0.94
26	2.56 ± 0.14 μM[b]	28.13 ± 1.14 μM	0.091	+	+	0.99	–	+	0.99
27	11.93 ± 0.61 μM	9.36 ± 0.26 μM	1.27	+	+	0.99	+	+	0.99
28	2.38 ± 0.06 μM[b]	1.49 ± 0.12 nM	1,597	+	+	0.99	+	+	0.99
29	255 ± 10.50 μM	260 ± 12.72 μM	0.98	–	+	0.91	–	+	0.92
30	12.20 ± 0.46 μM	16.53 ± 0.74 μM	0.74	+	+	0.92	+	+	0.61
31	57.92 ± 2.24 μM	**	<0.58[d]	–	+	0.87	–	+	0.87
32	32.80 ± 1.61 μM[b]	73.20 ± 4.23 μM	0.45	–	+	0.68	–	–	0.37
33	**	**	–	–	+	0.71	–	+	0.68
clorgyline	4.46 ± 0.32 nM[b]	61.35 ± 1.13 μM	0.00007	+	+	0.82	–	–	0.77
selegiline	67.25 ± 1.02 μM[b]	19.60 ± 0.86 nM	3431	–	–	0.33	+	+	0.99
iproniazide	6.56 ± 0.76 μM	7.54 ± 0.36 μM	0.87	+	+	0.79	+	+	0.82
moclobemide	361 ± 19.37 μM	*	<0.36[d]	–	–	0.42	–	–	0.92

[a] Each IC_{50} value is the mean ± SEM from five experiments ($n = 5$). * Inactive at 1 mM (highest concentration tested). ** Inactive at 100 μM (highest concentration tested). At higher concentrations, the compounds precipitate. *** Inactive at 50 μM (highest concentration tested). At higher concentrations the compounds precipitate. [b] Level of statistical significance:[b]$P < 0.01$ or [b]$P < 0.05$ versus the corresponding IC_{50} values obtained against MAO-B as determined by ANOVA/Dunnett's. [c] Level of statistical significance:[b]$P < 0.01$ or [b]$P < 0.05$ versus the corresponding IC_{50} values obtained against MAO-B as determined by ANOVA/Dunnett's. [d] Values obtained under the assumption that the corresponding IC_{50} against MAO-A/B is the highest concentration tested. [e] P Subsequent probability predicted by the model. [f] Observed and predicted groups for the selected compounds: (+) if the $IC_{50} < 25$ μM for the observed group, and if $P > 0.5$ for predicted group.

NMR ($CDCl_3$) 26.62 (Me-CO), 56.10 (MeO), 72.84 (CH_2O), 93.31 (C8), 95.27 (*C*6), 104.70, 111.67 (C3), 138.61 (C4), 156.61, 157.24, 161.27, 161.47 (*C*2), 203.30 (Me-CO). IR 3010, 1728, 1614, 1365, 1122, 1065, 816; MS *m/z* 249 ($[M + 1]^+$, 14), 248 (M^+, 100), 220 (3), 205 (74), 191 (3), 177 (47). Anal. ($C_{13}H_{12}O_5$) C, H.

8-Methoxy-4-methyl-7-(2′-oxocyclopentyloxy)coumarin (13). Yield 96%; mp 174−176 °C. ^{1}H NMR ($CDCl_3$) 1.88−2.55 (m, 6H (CH_2)$_3$), 2.39 (d, $J = 1.1$, 3H, Me), 3.97 (s, 3H, MeO), 4.77 (t, $J = 8.6$, 1H, H-1′), 6.17 (d, $J = 1.1$, 1H, H-3), 6.99 (d, $J = 8.9$, 1H, H-6), 7.27 (d, $J = 8.9$, 1H, H-5). ^{13}C NMR ($CDCl_3$) 17.25 (C4′), 18.78 (Me-C4), 29.58 (C5′), 35.23 (C3′), 61.57 (MeO), 80.81 (C1′), 112.39 (C3), 112.87 (C6), 115.86, 119.24 (C5), 137.47, 147.97, 152.50, 153.76 (C4), 160.52 (C2), 213.10 (C2′). IR 2994, 2932, 1755, 1718, 1604, 1300, 1114, 850. MS *m/z* 289 ($[M + 1]^+$, 15), 288 (M^+, 100), 231 (19), 205 (65), 178 (56). Anal. ($C_{16}H_{16}O_5$) C, H.

4,8-Dimethyl-7-(2′-oxocyclopentyloxy)coumarin (14). Yield 90%; mp 187 °C. ^{1}H NMR ($CDCl_3$) 2.09 (m, 4H, CH(CH_2)$_2$), 2.31 (s, 3H, Me-C8), 2.39 (d, $J = 1.1$, 3H, Me-C4), 2.47 (m, 2H, H-3′), 4.70 (t, $J = 7.8$, 1H, H-1′), 6.14 (d, $J = 1.1$, 1H, H-3), 6.94 (d, $J = 8.8$, 1H, H-6), 7.39 (d, $J = 8.8$, 1H, H-5). ^{13}C NMR ($CDCl_3$) 8.40 (Me-C8), 17.26 (Me-C4), 18.70 (C4′), 29.67 (C5′), 35.24 (C3′), 79.97 (C1′), 109.52 (C3), 112.12 (C6), 114.35 (C8), 115.15, 122.28 (C5), 152.64, 152.74, 158.69, 161.52 (C2), 213.41 (C2′). IR 2922, 1722, 1605, 1288, 1119; MS *m/z* 273 ($[M + 1]^+$, 16), 272 (M^+, 92), 201 (32), 190 (90), 162 (100), 115 (26). Anal. ($C_{16}H_{16}O_4$) C, H.

4,8-Dimethyl-7-(2′-oxocyclohexyloxy)coumarin (15). Yield 96%; mp 187−189 °C. ^{1}H NMR ($CDCl_3$) 1.80−2.70 (m, 8H (CH_2)$_4$), 2.37 (s, 6H, Me-C4, Me-C8), 4.73 (dd, $J = 5.2$, 9.2, 1H, H-1′), 6.14 (d, $J = 1.1$, 1H, H-3), 6.62 (d, $J = 8.8$, 1H, H-6), 7.33 (d, $J = 8.8$, 1H, H-5). ^{13}C NMR ($CDCl_3$) 8.9 (Me-C8), 19.0 (Me-C4), 23.1, 28.1, 34.9, 40.7, 81.5 (C1′), 109.3 (C3), 112.6 (C6), 114.6, 115.4, 122.6 (C5), 152.9, 153.2, 158.7, 161.8 (C2), 207.9 (C2′). IR 2945, 1727, 1706, 1598, 1283, 1119, 804. MS *m/z* 287 ($[M + 1]^+$, 7), 286 (M^+, 37), 190 (75), 162 (100), 115 (16). Anal. ($C_{17}H_{18}O_4$) C, H.

7-Acetonyloxy-3,4-cyclopentene-8-methylcoumarin (21). Yield 76%; mp 144 °C. ^{1}H NMR ($CDCl_3$) 2.18 (m, 2H, $CH_2CH_2CH_2$), 2.34 (s, 3H, MeCO), 2.38 (s, 3H, Me-C8), 2.87 (t, $J = 7.5$, 2H), 3.01 (t, $J = 5.9$, 2H), 4.63 (s, 2H, CH_2O), 6.64 (d, $J = 8.6$, 1H, H-6), 7.21 (d, $J = 8.6$, 1H, H-5). ^{13}C NMR ($CDCl_3$) 9.01 (Me-C8), 22.86 ($CH_2CH_2CH_2$), 27.10 (MeCO), 30.76, 32.40, 73.74 (CH_2O), 107.73 (C6), 113.69, 114.87, 122.98 (C5), 125.29, 153.72, 156.73, 157.98, 160.78 (C2), 205.29 (Me*C*O). IR 2956, 1733, 1706, 1615, 1376, 1286, 1120, 805. MS *m/z* 273 ($[M + 1]^+$, 18), 272 (M^+, 100), 229 (46), 215 (43), 187 (33), 128 (44). Anal. ($C_{16}H_{16}O_4$) C, H.

7-Acetonyloxy-3,4-cyclohexene-8-methylcoumarin (22). Yield 79%; mp 161−162 °C. ^{1}H NMR ($CDCl_3$) 1.81 (m, 4H, $CH_2(CH_2)_2CH_2$), 2.33 (s, 3H, MeCO), 2.37 (s, 3H, Me-C8), 2.54 (m, 2H), 2.72 (m, 2H), 4.62 (s, 2H, CH_2O), 6.64 (d, $J = 8.8$, 1H, H-6), 7.34 (d, $J = 8.8$, 1H, H-5). ^{13}C NMR ($CDCl_3$) 8.39 (Me-

C8), 21.43, 21.67, 23.89, 25.21, 26.70 (MeCO), 73.40 (CH_2O), 107.18 (C6), 114.24 (C8), 114.79, 120.97, 121.08 (C5), 147.13, 151.22, 157.09, 162.05 (C2), 205.13 (MeCO). IR 2942, 1738, 1698, 1605, 1416, 1292, 1025, 803. MS *m/z* 287 ([M + 1]$^+$, 38), 286 (M$^+$, 100), 271 (12), 258 (5), 243 (60), 230 (21). Anal. ($C_{17}H_{18}O_4$) C, H.

7-(*β*-Bromoallyloxy)-3,4-cyclopentene-8-methylcoumarin (24). Yield 78%; mp 140 °C. ^{1}H NMR ($CDCl_3$) 2.19 (m, 2H, $CH_2CH_2CH_2$), 2.38 (s, 3H, Me-C8), 2.90 (t, *J* = 7.5, 2H, CH_2−C4), 3.03 (t, *J* = 7.6, 2H, CH_2−C3), 4.72 (s, 2H, CH_2O), 5.71 (d, *J* = 2.1, 1H, C=CH), 6.01 (d, *J* = 2.1, 1H, C=CH), 6.77 (d, *J* = 8.6, 1H, H-6), 7.23 (d, *J* = 8.6, 1H, H-5). ^{13}C NMR ($CDCl_3$) 8.61 (Me-C8), 22.56 ($CH_2CH_2CH_2$), 30.40 (CH_2−C4), 32.07 (CH_2−C3), 72.02 (CH_2O), 108.09 (C6), 113.26 (C8), 114.81, 118.00 (CH_2=C), 122.47 (C5), 124.94, 126.52, 153.40, 156.40, 157.63, 160.58 (C2). IR 2919, 1716, 1611, 1373, 1282, 1109, 803. MS *m/z* (%): 336 ([M + 2]$^+$, 12), 335 (M$^+$, 12), 255 (76), 215 (29), 187 (100), 128 (15). Anal. ($C_{16}H_{15}BrO_3$) C, H.

7-(*β*-Bromoallyloxy)-3,4-cyclohexene-8-methylcoumarin (25). Yield 76%; mp 135−136 °C. ^{1}H NMR ($CDCl_3$) 1.82 (m, 4H, $CH_2(CH_2)_2CH_2$), 2.35 (s, 3H, Me-C8), 2.56 (m, 2H, CH_2−C4), 2.72 (m, 2H, CH_2−C3), 4.71 (s, 2H, CH_2O), 5.76 (d, *J* = 1.6, 1H, C=CH), 6.01 (d, *J* = 1.6, 1H, C=CH), 6.75 (d, *J* = 8.8, 1H, H-6), 7.35 (d, *J* = 8.8, 1H, H-5). ^{13}C NMR ($CDCl_3$) 8.78 (Me-C8), 21.86 (CH_2−CH_2C3), 22.11 (CH_2−CH_2C4), 24.31 (CH_2−C3), 25.65 (CH_2−C4), 72.36 (CH_2O), 108.32 (C6), 114.80 (C8), 115.04, 118.36 (CH_2=C), 121.26, 121.35 (C5), 127.03, 147.64, 151.57, 157.47, 162.60 (C2). IR 3071, 2935, 1708, 1605, 1114, 755. MS *m/z* 350 ([M + 2]$^+$, 4), 349 (M$^+$, 22), 269 (89), 229 (100), 201 (58), 187 (40). Anal. ($C_{17}H_{17}BrO_3$) C, H.

General Procedure for the Preparation of 3,4-Benzocoumarins 26−28. To a solution of the acyclic ether **22**, **23**,[45] or **25** (0.30 mmol) in toluene (15 mL) was added DDQ (0.60 mmol). The solution was heated under reflux for 5 h. The mixture was cooled, the precipitate filtered off, and the solvent evaporated under reduced pressure. The resulting residue was purified by FC to give the desired compound.

3,4-Benzo-7-acetonyloxy-8-methylcoumarin (26). Yield 64%; mp 172−174 °C. ^{1}H NMR ($CDCl_3$) 2.35 (s, 6H, Me-C8, MeCO), 4.60 (s, 2H, CH_2O), 6.63 (d, *J* = 8.8, 1H, H-6), 7.46 (m, 1H, CH-CHC3), 7.73 (m, 2H, H-5, CH-CHC4), 7.91 (d, *J* = 8.0, 1H, CH C4), 8.28 (d, *J* = 7.9, 1H, CH-C3). ^{13}C NMR ($CDCl_3$) 8.45 (Me-C8), 26.67 (MeCO), 73.19 (CH_2O), 107.43 (C6), 111.95, 114.95, 119.72, 120.44 (CH-C4), 121.12 (CH-CHC3), 127.72 (C5), 130.19 (CH-C3), 134.60 (CH-CHC4), 134.94, 150.15, 156.95, 161.13 (C2), 204.98 (MeCO). IR 2925, 1716, 1607, 1468, 1284, 1125, 766. MS *m/z* 283 ([M + 1]$^+$, 18), 282 (M$^+$, 100), 239 (60), 225 (43), 181 (51), 152 (47). Anal. ($C_{17}H_{14}O_4$) C, H.

3,4-Benzo-7-acetonyloxy-8-methoxycoumarin (27). Yield 56%; mp 172−174 °C. ^{1}H NMR ($CDCl_3$) 2.33 (s, 3H, MeCO), 4.05 (s, 3H, MeO), 4.72 (s, 2H, CH_2O), 6.80 (d, *J* = 9.0, 1H, H-6), 7.53 (t, *J* = 8.1, 1H, CH-CHC3), 7.70 (d, *J* = 9.0, 1H, H-5), 7.78 (t, *J* = 7.7, 1H, CH-CHC4), 7.99 (d, *J* = 8.0, 1H, CH-C4), 8.36 (d, *J* = 7.9, 1H, CH-C3). ^{13}C NMR ($CDCl_3$) 27.01 (MeCO), 62.15 (MeO), 74.62 (CH_2O), 110.94 (C6), 114.12, 118.00 (CH-C4), 120.50, 121.88 (C5), 128.76 (CH-CHC3), 131.04 (CH-C3), 135.29, 135.36 (CH-CHC4), 137.94, 146.26, 152.78, 161.07 (C2), 205.12 (MeCO). IR 2935, 1730, 1608, 1475, 1304, 1121, 812. MS *m/z* 299 ([M + 1]$^+$, 18), 298 (M$^+$, 100), 255 (27), 241 (67), 197 (25), 170 (19). Anal. ($C_{17}H_{14}O_5$) C, H.

3,4-Benzo-7-(*b*-bromoallyloxy)-8-methylcoumarin (28). Yield 82%; mp 128 °C. ^{1}H NMR ($CDCl_3$) 2.38 (s, 3H, Me-C8), 4.72 (s, 2H, CH_2O), 5.72 (d, *J* = 1.9, 1H, C=CH), 6.03 (d, *J* = 1.9, 1H, C=CH), 6.80 (d, *J* = 8.8, 1H, H-6), 7.49 (m, 1H, CH-CHC4), 7.78 (m, 1H + 1H, CH-CHC3 + H-5), 7.98 (d, *J* = 8.0, 1H, CH-C3), 8.34 (d, *J* = 8.0, 1H, CH-C4). ^{13}C NMR ($CDCl_3$) 8.95 (Me-C8), 72.33 (CH_2O), 108.68 (C6), 112.36, 115.67, 118.39 (C=CH_2), 120.25, 120.84 (CH−C4), 121.63 (CH-CHC3), 127.01, 128.18 (C5), 130.75 (CH-CHC4), 135.12 (CH−C3), 135.57, 150.66, 157.49, 161.78 (C2). IR 2921, 1726, 1608, 1470, 1283, 1115, 891, 766. MS *m/z* 347 ([M + 2]$^+$, 2), 345 (M$^+$, 12), 344 (13), 265 (60), 225 (100), 171 (17). Anal. ($C_{17}H_{13}BrO_3$) C, H.

General Procedure for the Preparation of the Furocoumarin derivatives 29, 32, 33. To a solution of the corresponding ketoether **11**, **14**, or **15** (3.39 mmol) in ethyl alcohol (200 mL) was added 0.1 M NaOH (200 mL). The mixture was heated under reflux for 12 h, acidified with HCl, and concentrated to half-volume and left overnight. The resulting precipitate was filtered off and purified by FC to give the desired compound.

5-Methoxy-4′-methylfuro[3,2-*g*]coumarin (29). Yield 70%; mp 140 °C, ^{1}H NMR ($CDCl_3$) 2.40 (d, *J* = 1.3, 3H, Me-C4′), 3.99 (s, 3H, MeO), 6.34 (d, *J* = 9.8, 1H, H-3), 7.21 (s, 1H, H-8), 7.37 (d, *J* = 1.3, 1H, H-5′), 8.06 (d, *J* = 9.8, 1H, H-4), ^{13}C NMR ($CDCl_3$) 9.26 (Me-C4′), 64.94 (MeO), 96.58 (C8), 109.20, 113.63 (C3), 114.68, 119.13, 138.57 (C4), 142.52 (C5′), 150.99, 152.35, 158.36, 161.04 (C2), IR 3110, 2945, 1732, 1717, 1634, 1607, 1113, 820, MS *m/z* 231 ([M + 1]$^+$, 14), 230 (M$^+$, 100), 215 (78), 187 (49), 159 (25), 131 (8). Anal. ($C_{13}H_{10}O_4$) C, H.

4′,5′-Cyclopentene-4,8-dimethylfuro[3,2-*g*]coumarin (32). Yield 30%; mp 153 °C, ^{1}H NMR ($CDCl_3$) 2.48 (s, 3H, Me-C8), 2.57 (s, 3H, Me-C4), 2.59 (m, 2H, $CH_2CH_2CH_2$), 2.78 (m, 2H, CH_2-C5′), 2.90 (m, 2H, CH_2-C4′), 6.24 (s, 1H, H-3), 7.41 (s, 1H, H-5). ^{13}C NMR ($CDCl_3$) 8.9 (Me-C8), 19.7 (Me-C4), 23.1 ($CH_2CH_2CH_2$), 25.6 (CH_2-C4′), 27.6 (CH_2-C5′), 110.6 (C8), 111.3 (C3), 113.2 (C5), 116.2, 121.7, 123.3, 148.9, 153.8, 161.4, 162.1, 164.9 (C2). IR 2922, 2850, 1706, 1558, 1480, 1396, 1125, 1092. MS *m/z* 254 (M$^+$, 80), 226 (M$^+$ − CO, 100), 225 (98), 199 (18), 183 (15), 149 (56). Anal. ($C_{16}H_{14}O_3$) C, H.

4′,5′-Cyclohexene-4,8-dimethylfuro[3,2-*g*]coumarin (33). Yield 56%; mp 189−190 °C. ^{1}H NMR ($CDCl_3$) 1.85−2.00 (m, 4H, $CH_2(CH_2)_2CH_2$), 2.50 (d, *J* = 1.1, 3H, Me-C4), 2.58 (s, 3H, Me-C8), 2.65 (m, 2H, CH_2-C5′), 2.78 (CH_2-C4′), 6.24 (d, *J* = 1.1, 1H, H-3), 7.41 (s, 1H, H-5). ^{13}C NMR ($CDCl_3$) 8.9 (Me-C8), 19.7 (Me-C4), 20.8 (CH_2-C5′), 22.8, 23.1, 23.9 (CH_2-C4′), 109.0 (C8), 110.7 (C3), 113.0 (C5), 113.3, 116.2, 126.3, 150.1, 152.0, 153.7, 156.3, 162.0 (C2). IR 3070, 2923, 1716, 1639, 1403, 1183, 1100, 873. MS *m/z* 269 ([M + 1]$^+$, 11), 268 (M$^+$, 100), 240 (29), 212 (19), 167 (13), 127 (10). Anal. ($C_{17}H_{16}O_3$) C, H.

Biological Assay. Enzymatic MAO-A and MAO-B activity of compounds was determined by a fluorimetric method following a previously described protocol.[41] Briefly, 0.1 mL of sodium phosphate buffer (0.05 M, pH 7.4) containing various concentrations of the test drugs (new compounds or reference inhibitors) and appropriate amounts of recombinant hMAO-A or hMAO-B (Sigma-Aldrich Quimica S.A., Alcobendas, Spain) and adjusted to obtain in our experimental conditions the same reaction velocity in the presence of both isoforms (i.e., to oxidize (in the control group) the same concentration of substrate: 165 pmol of *p*-tyramine/min (hMAO-A: 1.1 *μ*g protein; specific activity: 150 nmol of *p*-tyramine oxidized to *p*-hydroxyphenylacetaldehyde/min/mg protein; hMAO-B: 7.5 *μ*g protein; specific activity: 22 nmol of *p*-tyramine transformed/min/mg protein) were incubated for 15 min at 37 °C in a flat-black-bottom 96-well microtest plate (BD Biosciences, Franklin Lakes, NJ) placed in the dark fluorimeter chamber. After this incubation period, the reaction was started by adding (final concentrations) 200 *μ*M of 10-acetyl-3,7-dihydroxyphenoxazine reagent (Amplex Red assay kit, Molecular Probes, Inc., Eugene, OR), 1 U/mL horseradish peroxidase, and 1 mM *p*-tyramine. The production of H_2O_2 and, consequently, of resorufin, was quantified at 37 °C in a multidetection microplate fluorescence reader (FLX800, Bio-Tek Instruments, Inc., Winooski, VT) based on the fluorescence generated (excitation, 545 nm, emission, 590 nm) over a 15 min period, during which the fluorescence increased linearly.

Control experiments were carried out simultaneously by replacing the test drugs (new compounds and reference inhibitors) with appropriate dilutions of the vehicles. In addition, the possible capacity of the above test drugs to modify the fluorescence generated in the reaction mixture due to nonenzymatic inhibition was determined by adding these drugs to solutions containing only the Amplex Red reagent in a sodium phosphate buffer.

To determine the kinetic parameters of hMAO-A and hMAO-B (K_m and V_{max}), the corresponding enzymatic activity of both isoforms was evaluated (under the experimental conditions described above) in the presence of a number of *p*-tyramine concentrations.

The specific fluorescence emission (used to obtain the final results) was calculated after subtraction of the background activity, which was determined from vials containing all components except the MAO isoforms, which were replaced by a sodium phosphate buffer solution.

Acknowledgment. We are grateful to the Xunta de Galicia (PGIDIT05PXIB20304PR, PGIDIT05BTF20302PR, and INCITE07PXI203039ES) and Ministerio de Sanidad y Consumo (FIS PI061537 and PI061457) for financial support.

Supporting Information Available: Table 1SI including the complete list of compounds used in training sets, an indication of the compound number in the corresponding bibliographic reference, the observed and predicted classification, and subsequent probabilities of a positive result predicted for each compound. Table 2SI with the factor scores (F_1 to F_{10}) for each compound. Table 3SI with the conditions in terms of enzyme, species and organs of all experimental results used as input for the QSAR model. Bibliographic references for database compounds. Elemental analysis data for synthesized compounds. Information from pharmacological studies. This material is available free of charge via the Internet at http://pubs.acs.org.

References

(1) Dostert, P.; Strolin Benedetti, M.; Jafre, M. Structural modifications in oxazolidinone series leading to type A or B selective monoamine oxidase inhibitors. In *Monoamine Oxidase: Basic and Clinical Frontiers*; Kamijo, K., Usdin, E., Nagausu, T., Eds.; Excerpta Medica: Amsterdam, 1982; pp 197−208.

(2) Singer, T. P. Monoamine oxidases. In *Chemistry and Biochemistry of Flavoenzymes (II)*; Muller, F., Ed.; CRC Press: London, 1991; pp 437−470.

(3) De Colibus, L.; Li, M.; Binda, C.; Lustig, A.; Edmondson, D. E.; Mattevi, A. Three-dimensional structure of human monoamine oxidase A (MAO A): relation to the structures of rat MAO A and human MAO B. *Proc. Natl. Acad. Sci. U.S.A.* **2005**, *102*, 12684–12689.

(4) Binda, C.; Li, M.; Hubálek, F.; Restelli, N.; Edmondson, D. E.; Mattevi, A. Insights into the mode of inhibition of human mitochondrial monoamine oxidase B from high-resolution crystal structures. *Proc. Natl. Acad. Sci. U.S.A.* **2003**, *100*, 9750–9755.

(5) Yamada, M.; Yasuhara, H. Clinical pharmacology of MAO inhibitors: safety and future. *Neurotoxicology* **2004**, *25*, 11–20.

(6) Rudorfer, M. V.; Potter, V. Z. Antidepressants. A comparative review of the clinical pharmacology and therapeutic use of the "newer" versus the "older" drugs. *Drugs* **1989**, *37*, 713–738.

(7) Palhagen, S.; Heinonen, E.; Hagglund, J.; Kaugesaar, T.; Maki-Ikola, O.; Palm, R. Selegiline slows the progression of the symptoms of Parkinson disease. *Neurology* **2006**, *66*, 1200–1206.

(8) Guay, D. R. Rasagiline (TVP-1012): a new selective monoamine oxidase inhibitor for Parkinson's disease. *Am. J. Geriatr. Pharmacother.* **2006**, *4*, 330–346.

(9) Riederer, P.; Danielczyk, W.; Grunblatt, E. Monoamine oxidase-B inhibition in Alzheimer′s desease. *Neurotoxicology* **2004**, *25*, 271–277.

(10) Youdim, M. B. H.; Fridkin, M.; Zheng, H. Novel bifunctional drugs targeting monoamine oxidase inhibition and iron chelation as an approach to neuroprotection in Parkinson's disease and other neurodegenerative diseases. *J. Neural Transm.* **2004**, *111*, 1455–1471.

(11) Cesura, A. M.; Pletscher, A. The new generation of monoamine oxidase inhibitors. *Prog. Drug Res.* **1992**, *38*, 171–297.

(12) Youdim, M. B. The advent of selective monoamine oxidase A inhibitor antidepressants devoid of the cheese reaction. *Acta Psychiatr. Scand., Suppl.* **1995**, *386*, 5–7.

(13) Edmondson, D. E.; Mattevi, A.; Binda, C.; Li, M.; Hubalek, F. Structure and mechanism of monoamine oxidase. *Curr. Med. Chem.* **2004**, *11*, 1983–1993.

(14) Tipton, K. F.; Boyce, S.; O'Sullivan, J.; Davey, G. P.; Healy, J. Monoamine oxidases: Certainties and uncertainties. *Curr. Med. Chem.* **2004**, *11*, 1965–1982.

(15) Edmondson, D. E.; Binda, C.; Mattevi, A. Structural insights into the mechanism of amine oxidation by monoamine oxidases A and B. *Arch. Biochem. Biophys.* **2007**, *464*, 269–276.

(16) Binda, C.; Hubalek, F.; Li, M.; Herzig, Y.; Sterling, J.; Edmondson, D. E.; Mattevi, A. Crystal Structures of Monoamine Oxidase B in Complex with Four Inhibitors of the *N*-Propargylaminoindane Class. *J. Med. Chem.* **2004**, *47*, 1767–1774.

(17) Chimenti, F.; Maccioni, E.; Secci, D.; Bolasco, A.; Chimenti, P.; Granese, A.; Befani, O.; Turini, P.; Alcaro, S.; Ortuso, F.; Cirilli, R.; La Torre, F.; Cardia, M. C.; Distinto, S. Synthesis, Molecular Modeling Studies, and Selective Inhibitory Activity against Monoamine Oxidase of 1-Thiocarbamoyl-3,5-diaryl-4,5-dihydro-(1*H*)-pyrazole Derivatives. *J. Med. Chem.* **2005**, *48*, 7113–7122.

(18) Harkcom, W. T.; Bevan, D. R. Molecular docking of inhibitors into monoamine oxidase B. *Biochem. Biophys. Res. Commun.* **2007**, *360*, 401–406.

(19) Gallardo-Godoy, A.; Fierro, A.; McLean, T. H.; Castillo, M.; Cassels, B. K.; Reyes-Parada, M.; Nichols, D. E. Sulfur-Substituted α-Alkyl Phenethylamines as Selective and Reversible MAO-A Inhibitors: Biological Activities, CoMFA Analysis, and Active Site Modeling. *J. Med. Chem.* **2005**, *48*, 2407–2419.

(20) Mevedev, A. E.; Veselovsky, A. V.; Shvedov, V. I.; Tikhonova, T. A.; Moskvitinia, T. A.; Fedotova, O. A.; Axenova, L. N.; Kamyshanskaya, A. Z.; Kirkel, A. Z.; Ivanov, A. Inhibition of Monoamino Oxidase by Pirlindole Analogues: 3D-QSAR and CoMFA Analysis. *J. Chem. Inf. Comput. Sci.* **1998**, *38*, 1137–1144.

(21) Chimenti, F.; Bolasco, A.; Manna, F.; Secci, D.; Chimenti, P.; Granese, A.; Befani, O.; Turini, P.; Cirilli, R.; La Torre, F.; Alcaro, S.; Ortuso, F.; Langer, T. Synthesis, biological evaluation and 3D-QSAR of 1,3,5-trisubstituted-4,5-dihydro-(1*H*)-pyrazole derivatives as potent and highly selective monoamine oxidase A inhibitors. *Curr. Med. Chem.* **2006**, *13*, 1411–1428.

(22) Gnerre, C.; Catto, M.; Francesco, L.; Weber, P.; Carrupt, P.-A.; Altomare, C.; Carotti, A.; Testa, B. Inhibition of Monoamine Oxidase by Functionalized Coumarin derivatives: Biological Activities, QSAR, and 3D-QSARs. *J. Med. Chem.* **2000**, *43*, 4747–4758.

(23) Nunez, M. B.; Maguna, F. P.; Okulik, N. B.; Castro, E. A. QSAR modeling of the MAO inhibitory activity of xanthone derivatives. *Bioorg. Med. Chem. Lett.* **2004**, *14*, 5611–5617.

(24) Todeschini, R.; Consonni, V. *Handbook of Molecular Descriptors*; Mannhold, R., Kubinyi, H., Timmerman, H., Eds.; Wiley-VCH: Weinheim, 2000.

(25) Kier, L. B.; Hall, L. H. The Kappa indices for modeling molecular shape and flexibility in *Topological Indices and Related Descriptors in QSAR and QSPR*; Devillers, J., Balaban, A. T., Eds.; Gordon and Breach Science Publishers: Amsterdam, 1999, pp 445−489.

(26) Estrada, E.; Uriarte, E.; Montero, A.; Teijeira, M.; Santana, L.; De Clercq, E. A Novel Approach for the Virtual Screening and Rational Design of Anticancer Compounds. *J. Med. Chem.* **2000**, *43*, 1975–1985.

(27) Erdem, S. S.; Karahan, O.; Yildiz, I.; Yelekci, K. A computational study on the amine-oxidation mechanism of monoamine oxidase: insight into the polar nucleophilic mechanism. *Chem. Org. Biomed. Chem.* **2006**, *4*, 646–658.

(28) Freund, J. A., Poschel, T. Eds. Stochastic Processes in Physics, Chemistry, and Biology. In *Lecture Notes in Physics*; Springer-Verlag: Berlin, Germany, 2000.

(29) González-Díaz, H.; Agüero, G.; Cabrera, M. A.; Molina, R.; Santana, L.; Uriarte, E.; Delogu, G.; Castañedo, N. Unified Markov thermodynamics based on stochastic forms to classify drugs considering molecular structure, partition system, and biologic species. Distribution of the antimicrobial G1 on rat tissues. *Bioorg. Med. Chem. Lett.* **2005**, *15*, 551–557.

(30) González-Díaz, H.; Cruz-Monteagudo, M.; Molina, R.; Tenorio, E.; Uriarte, E. Predicting multiple drugs side effects with a general drug−target interaction thermodynamic Markov model. *Bioorg. Med. Chem.* **2005**, *13*, 1119–1129.

(31) González-Díaz, H.; Torres-Gómez, L. A.; Guevara, Y.; Almeida, M. S.; Molina, R.; Castañedo, N.; Santana, L.; Uriarte, E. Markovian chemicals "in silico" design (MARCH-INSIDE), a promising approach for computer-aided molecular design III: 2.5D indices for the discovery of antibacterials. *J. Mol. Model.* **2005**, *11*, 116–123.

(32) Santana, L.; Uriarte, E.; González-Díaz, H.; Zagotto, G.; Soto-Otero, R.; Méndez-Alvarez, E. A QSAR Model for in Silico Screening of MAO-A Inhibitors. Prediction, Synthesis, and Biological Assay of Novel Coumarins. *J. Med. Chem.* **2006**, *49*, 1149–1156.

(33) Fierro, A.; Osorio-Olivares, M.; Cassels, K.; Edmondson, D. E.; Sepulveda-Boza, S.; Reyes-Parada, M. Human and rat monoamine oxidase-A are differentially inhibited by (*S*)-4-alkylthioamphetamine derivatives: insights from molecular modeling studies. *Bioorg. Med. Chem.* **2007**, *15*, 5198–5206.

(34) Novaroli, L.; Daina, A.; Favre, E.; Bravo, J.; Carotti, A.; Leonetti, F.; Catto, M.; Carrupt, P. A.; Reist, M. Impact of Species-Dependent Differences on Screening, Design, and Development of MAO-B Inhibitors. *J. Med. Chem.* **2006**, *49*, 6264–6272.

(35) Van Waterbeemd, H. Discriminant analysis for activity prediction. In *Chemometric Methods in Molecular Design. Method and Principles in Medicinal Chemistry*, Vol. 2; Wiley-VCH: Weinhiem, 1995; pp 265−282.
(36) Kleeman, A.; Engel, J.; Kutscher, B.; Reichert, D. *Pharmaceutical Substances: Syntheses, Patents and Applications*, 4th Ed.; George Thieme Verlag: Stuttgart, 2001.
(37) Negwer, M. *Organic Chemical Drugs and their Synonyms: An International Survey*; Akademie-Verlag: Berlin, 1987.
(38) Iding, H.; Jolidon, S.; Krummenacher, D.; Rodriguez Sarmiento, R. M.; Thomas, A. W.; Wirz, B.; Wostl, W.; Wyler, R. (F. Hoffmann-La Roche A.-G., Switzerland). Preparation of arylpyrrolidones as monoamine oxidase-B (MAO-B) inhibitors. Patent WO 2004026825 A1, 2004.
(39) Jolidon, S.; Rodriguez-Sarmiento, R. M.; Thomas, A. W.; Wostl, W.; Wyler, R. (F. Hoffmann-La Roche A.-G., Switzerland). Preparation of 4-pyrrolidinophenyl benzyl ether derivatives as monoamine oxidase B inhibitors. Patent WO 2004026826 A1, 2004.
(40) Borges, F.; Roleira, F.; Mihazes, N.; Santana, L.; Uriarte, E. Simple coumarins and analogues in medicinal chemistry: occurrence, synthesis and biological activity. *Curr. Med. Chem,* **2005**, *12*, 887–916.
(41) Chimenti, F.; Secci, D.; Bolasco, A.; Chimenti, P.; Granese, A.; Befani, O.; Turini, P.; Alcaro, S.; Ortuso, F. Inhibition of monoamine oxidases by coumarin-3-acyl derivatives: biological activity and computational study. *Bioorg. Med. Chem. Lett.* **2004**, *14*, 3697–3703.
(42) Catto, M.; Nicolotti, O.; Leonetti, F.; Carotti, A.; Soto-Otero, R.; Mendez-Alvarez, E.; Carotti, A. Structural Insights into Monoamine Oxidase Inhibitory Potency and Selectivity of 7-Substituted Coumarins from Ligand- and Target-Based Approaches. *J. Med. Chem.* **2006**, *49*, 4912–4925.
(43) Binda, C.; Wang, J.; Pisani, L.; Caccia, C.; Carotti, A.; Salvati, P.; Edmondson, D. E.; Mattevi, A. Structures of Human Monoamine Oxidase B Complexes with Selective Noncovalent Inhibitors: Safinamide and Coumarin Analogs. *J. Med. Chem.* **2007**, *50*, 5848–5852.
(44) Carotti, A.; Altomare, C.; Catto, M.; Gnerre, C.; Summo, L.; De Marco, A.; Rose, S.; Jenner, P.; Testa, B. Lipophilicity Plays a Major Role in Modulating the Inhibition of Monoamine Oxidase B by 7-Substituted Coumarins. *Chem. Biodiversity* **2006**, *3*, 134–149.
(45) Dalla Via, L.; Uriarte, E.; Quezada, E.; Dolmella, A. M. G.; Ferlin, M. G.; Gia, O. Novel Pyrone Side Tetracyclic Psoralen Derivatives: Synthesis and Photobiological Activity. *J. Med. Chem.* **2003**, *46*, 3800–3810.
(46) Gia, O.; Marciani-Magno, S.; González-Díaz, H.; Quezada, E.; Santana, L.; Uriarte, E.; Dalla Via, L. Design, Synthesis and Photobiological Properties of 3,4-Cyclopentene Psoralens. *Bioorg. Med. Chem.* **2005**, *13*, 809–817.
(47) Dalla Via, L.; Uriarte, E.; Santana, L.; Marciani-Magno, S.; Gia, O. Methyl derivatives of tetracyclic psoralen analogues: antiproliferative activity and interaction with DNA. *ARKIVOC* **2004**, *5*, 131–146.
(48) Yáñez, M.; Fraiz, N.; Cano, E.; Orallo, F. Inhibitory effects of *cis*- and *trans*-resveratrol on noradrenaline and 5-hydroxytryptamine uptake and on monoamine oxidase activity. *Biochem. Biophys. Res. Commun.* **2006**, *344*, 688–695.
(49) González-Díaz, H.; Molina-Ruiz, R.; Hernandez, I. *MARCH-INSIDE (MARkov CHains INvariants for SImulation & DEsign)*, version 3.0. Windows supported version released under request to the main author. Contact E-mail: humberto.gonzalez@usc.es.
(50) *Statistica Software*, version 8.0; StatSoft Iberica Portugal Lda.: Lisboa, Portugal, 2008.
(51) Junker, B. H.; Koschützki, D.; Schreiber, F. Exploration of biological network centralities with CentiBiN. *BMC Bioinform.* **2006**, *7*, 219.
(52) Batagelj, V.; Mrvar, A. *Pajek: Program for Large Network Analysis*. Home page: http://vlado.fmf.uni-lj.si/pub/networks/pajek/.

JM800656V